

Synthesis and Characterization of Poly (Acrylamide - co - Acrylic acid) Hydrogel Containing Silver Nanoparticles for Antimicrobial Applications

Fatma S. Aggor¹; Enas M. Ahmed^{1*}, A.T. El-Aref² and M. A. Asem³

¹ Department of Chemical Engineering & Pilot Plant ² Department of Pre-treatments and Finishing.

³ Department of Chemistry of Natural and Microbial Products, National Research Center, Dokki, Cairo, Egypt
^{*}elarefenas123@yahoo.com

Abstract: Acrylamide was copolymerized with acrylic acid at different ratios using potassium persulphate initiation system in presence of a crosslinking agent and different doses of silver nitrate to yield hydrogels containing silver nanoparticles upon post treatment with sodium hydroxide. Swelling capacity and kinetics of swelling of these hydrogels were studied. Size and distribution of the nanoparticles and their dependence on acrylamide / acrylic acid ratios as well as on the dose of silver nitrate were also studied using Transmission Electron Microscopy (TEM). Furthermore, the antimicrobial and antifungal activities of the hydrogels in correlation with TEM results were reported. Hydrogels samples having relatively large number of Ag nanoparticles and widely distributed smaller particle size inhibit bacterial and fungal growth.

[Fatma S. Aggor; Enas M. Ahmed, A.T. El-Aref and M. A. Asem. **Synthesis and Characterization of Poly (Acrylamide - co - Acrylic acid) Hydrogel Containing Silver Nanoparticles for Antimicrobial Applications.** Journal of American Science 2010;6(12):648-656]. (ISSN: 1545-1003). <http://www.americanscience.org>.

Key words: hydrogel; silver nanoparticles; kinetic study; antimicrobial activity.

1. Introduction:

By definition, hydrogels represent polymeric networks capable of absorbing large quantities of water, but remain insoluble due to chemical or physical crosslinks between individual polymeric chains [1]. Recently, there is a great deal of interest concerning the production of nanoparticles in the hydrogel networks since they have enormous valuable applications in bio-related fields [2]. Indeed the design and development of nanoparticles and nanostructural materials have opened a new era for constructing well designed nanostructures that have been considered as a novel class of materials for catalytic, optical, electronic and biomedical application.

Previous studies concerned with metal nanoparticles especially those of silver, gold and copper were found to exhibit resistance to microorganisms [3, 4]. It was also reported that among these nanoparticles, nanosilver displayed acceptable antimicrobial properties [5, 6]. Nanosilver particles were introduced to a wide range of medical applications and water purifying systems [7, 8]. Silver nanoparticles proved to be non-toxic and eco-friendly antibacterial agents. The problem of their weak binding properties was overcome via preparation of stabilized nanoparticles in a polymer, notably hydrogel networks where the nanoparticles were embedded therein [9, 10].

Gels of importance are of polymeric nature due to the possibilities they offer to design systems with well defined and controlled properties. Silver and

silver ions have long been known to have strong inhibitory and anti bacterial effects as well as a broad spectrum of antimicrobial activities [11]. But silver is expensive and the antibiotic introduction in the last century made it out of use. In recent years, however, the nanoscale techniques were developed for producing silver nanoparticles which may assist the medical use resurgence of silver, especially in applications where fighting germs is a concern.

Silver nanoparticles, which have a high specific surface area and a high fraction of surface atoms, have attracted the attention of the industry because of their unique characteristics, high efficiency and antimicrobial activity, even at low concentrations [12, 13]. The exact antimicrobial mechanism of silver is not well established; however, it was reported that the free silver ion is the active agent, combining the thiol (SH) groups, which leads to the protein inactivation [14]. There is evidence that antibacterial potency of silver is directly proportional to the concentration of silver ions in the medium [15–16].

Polymer nanocomposite containing metal nanoparticles can be prepared by several methods. Methods used for preparation comprise mechanical mixing of a polymer with metal nanoparticles, the in situ polymerization of a monomer in the presence of metal nanoparticles and the in situ reduction of metal salts or in a polymer [17]. Copolymeric hydrogel networks are composed of two or more different monomer species with at least one hydrophilic component, arranged in a random, block or alternating configuration along the chain of the

polymer network. The copolymeric hydrogel networks are generally covalently or ionically crosslinked structures, which are not water soluble.

In the present work, in situ synthesis of silver nanoparticles within swollen hydrogel networks is undertaken. Thus, copolymer gels were prepared by simultaneous polymerization of acrylamide (AAM) and acrylic acid (AAc) using potassium persulphate (KPS) as free radical initiator and N,N'-methylenebisacrylamide (MBA) as crosslinking agent in presence of silver nitrate. Swelling behavior and swelling kinetics of the so obtained hydrogels were evaluated. Distribution of the silver nanoparticles through their characterization within the hydrogels using TEM was studied. Also studied were the antibacterial and antifungal activities of the hydrogels under investigation.

2. Experimental

2.1. Materials

Acrylamide (AAM) and acrylic acid (AAc) in the monomeric form were provided by Sisco Research Lab. PVT. LTD, India; while N,N'-methylenebisacrylamide (MBA), crosslinking agent, potassium persulphate (KPS), initiator and silver nitrate (AgNO₃) were supplied by Sigma – Aldrich, Inc. These reagents were used as laboratory grade chemicals.

Escherichia coli NRRL B-210 (Gram -ve bacteria), *Bacillus subtilis* NRRL B-543 and *Staphylococcus aureus* (Gram +ve bacteria), *Candida albicans* NRRL Y-477 (Fungi) were obtained from Northern Utilisation Research and Development Division, U.S. Department of Agricultural Peoria, Illinois, USA.

2.2. Procedures

2.2.1. Preparation of Ag nanoparticles

Hydrogel loaded with silver nanoparticles were prepared according to the procedure described elsewhere [17]. The hydrogel disks were prepared by free radical aqueous copolymerization of AAM and AAc in presence of MBA as crosslinker and KPS for initiating the polymerization system. A weighed amount of AgNO₃ was dissolved in double distilled water; desired amounts of AAM/AAc and MBA were added and the final volume was made 10 ml. A certain amount of KPS was dissolved and the whole reaction mixture was transferred to the test tube and then heated gently up to 70°C for 30 minutes. The test tube was broken and the resulting hydrogels were cut into slices of same thickness and then washed thoroughly with double distilled water. The hydrogel was then added to an aqueous solution of NaOH (5 wt %), and kept overnight till complete reduction of

Ag⁺ ions as indicated by faint yellow color of the colloidal Ag nanoparticles within the hydrogel network, washed several times in double distilled water and kept therein till complete swelling.

Blank experiment (omitting Ag⁺ ions) and Ag/PAAM/AAc hydrogel prepared using different molar ratios of AAM/ Ag⁺ ions were also performed. The prepared hydrogels were air-dried followed by vacuum drying and kept for characterization. Table I contains the monomers ratios and silver nitrate doses used throughout nanosilver hydrogel composite preparation.

Table I: Monomers ratio and silver nitrate dose.

Sample	AAM/AAc Ratio (g/g)	Silver nitrate dose (g/g monomer mixture)
HG ₀ (Blank)	50/50	-----
HG ₁	100/0	0.01
HG ₂	70/30	0.01
HG ₃	50/50	0.01
HG ₄	30/70	0.01
HG ₅	0/100	0.01
HG ₆	50/50	0.02
HG ₇	50/50	0.03
HG ₈	50/50	0.04

1.3. Characterization

2.3.1. Swelling studies

The swelling characteristics of the prepared hydrogel were measured through gravimetric analysis [18]. The dried samples were placed in 50 ml of distilled water at room temperature (25 ± 1 °C) and taken from water at regular time intervals. The surface water on the swollen hydrogel was removed by soft pressing the sample between the folds of a filter paper; an increase in weight was recorded. The swelling equilibrium of the gels was determined as follows: gels were dried for a day at room temperature and were then dried in vacuum at 60°C. After the weight of the dried samples was determined, the samples were equilibrated in distilled water for 3 days at room temperature and then weighed again. The swelling ratio (S) and equilibrium swelling ratio (S_{eq}) were determined and calculated by application in the following equations [17]:

$$S(g/g) = \frac{W_t - W_o}{W_o} \quad (1)$$

$$S_{eq}(g/g) = \frac{W_{eq} - W_o}{W_o} \quad (2)$$

Where, W_o, W_t, and W_{eq} are the weights of the

samples in the dry state, the swollen state at a certain time, and the completely (equilibrium) swollen state, respectively.

2.3.2. Antimicrobial assay

The prepared hydrogel samples were screened in vitro for their antimicrobial activities against *Escherichia coli* NRRL B-210 (Gram -ve bacteria), *Bacillus subtilis* NRRL B-543 and *Staphylococcus aureus* (Gram +ve bacteria), *Candida albicans* NRRL Y-477 (Fungi).

The agar diffusion method [19] was used for this purpose. Bacteria and fungi were maintained on nutrient agar and Czapek's-Dox agar media, respectively. The assay medium flasks containing 50 ml of nutrient agar for bacteria and Czapek's-Dox agar medium for fungi respectively were allowed to reach 40-50°C to be incubated with 0.5ml of the test organism cell suspension.

The flasks were mixed well and poured each into a Petri dish (15 x 2 cm) and allowed to solidify. After solidification, holes (6 mm diameter) were made in the agar plate by the aid of a sterile cork poorer. The prepared hydrogel samples were cut to small pieces and allowed to swallow using sterile distilled water then left on agar surface. The Petri dishes were kept at 5°C for 1 hour to allow diffusion of the samples through the agar medium and retard the growth of the test organism. Plates were incubated at 30 °C for 24 hours for bacteria and 72 h of incubation at 28 °C for fungi. The diameter of the resulted inhibition zone was measured in mm [19].

2.3.3. Transmission Electron Microscopy (TEM)

Images for the blank hydrogel and nanosilver hydrogel composites were recorded using a JEOL JEM-1230 electron microscope operating at an acceleration voltage of 100 kV. Specimens for TEM were prepared by the placement of a swollen sample of hydrogel on a 400-mesh copper grid followed by evaporation of excess water in air under ambient conditions (25 ± 1°C).

3. Results and Discussion

The concept of producing nanoparticles in the networks of hydrogel systems was recognized as an important approach due to its direct applicability in various biomedical applications. That is why, a number of composite systems were evaluated [20]. The P(AAm-co-AAc)/silver nanoparticles hydrogels prepared as described above were investigated. In accordance with previous reports [17] the free network spaces between hydrogel networks reserve and stabilize nanoparticles. Moreover, the in situ reduction of metal ions and the stabilization of particles can be verified by the following: (a) metal

ions are attached to reactive sites of hydrogel networks, and larger amounts of these ions are embedded in the network spaces of hydrogels; (b) the reduction process proceeds under the action of sodium hydroxide; and (c) the resulting particles are well stabilized through the hydrogel network interspaces.

3.1. Swelling behaviour

Swelling experiments were carried out with a view of evaluation the swelling capacity of the hydrogels under investigation in distilled water. Results of these experiments indicated that the increase in weight of the swollen hydrogels is directly related to the duration of swelling. The swelling behaviour observed could be associated with the absorption mechanism, which, in turn, is determined by the diffusion process.

Figure 1 illustrates the effect of AAm /AAc ratio in presence of silver nanoparticles on the swelling characteristics of the prepared hydrogel. It is evident that the swelling ratio increases sharply upon prolongation of swelling time up to ca 60 minutes then levels off. It was also observed that the swellability of the prepared hydrogel increases at higher concentrations of Polyacrylic acid (PAAc) ratio in the matrix. This is expected since abundance of the hydrophilic groups of AAac causes an improvement in the swelling characteristics of the hydrogel prepared under these conditions.

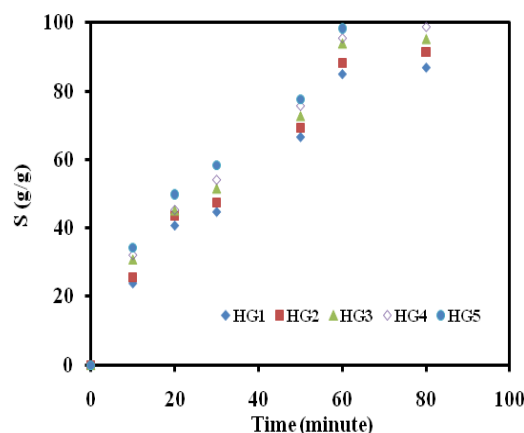


Figure 1: Effect of variation in AAm/AAc ratio on the swelling behavior of P(AAm-co-AAc)/silver nanoparticles hydrogel at different swelling durations

3.2. Kinetic study of swelling

The swelling kinetics of the prepared hydrogel was undertaken with view of clarifying the controlling mechanism of the swelling processes. This was visualized through kinetic models. The

latter were used to examine the results concerning swelling efficiency of the prepared hydrogels at different durations derived from the experimental work. A simple kinetic analysis represented by a second-order equation was applied in this study using the following relationship [17]:

$$\frac{dS}{dt} = k_s (S_{eq} - S)^2 \quad (3)$$

Where:

k_s is the swelling rate constant and,
 S_{eq} is the degree of swelling at the state of equilibrium.

After integration, when the initial conditions $S = 0$ at $t = 0$ and $S = S$ at $t = t$, are applicable, equation (3) is modified to be as follows:

$$\frac{t}{S} = A + Bt \quad (4)$$

Where

$A = 1/k_s \cdot S_{eq}^2$ is the reciprocal of the rate of swellin at the initial state $[(dS/dt)_0]$ of the hydrogel, $B = 1/S_{eq}$ is the inverse of the maximum or equilibrium swelling and, k_s represents the swelling rate constant.

The kinetic models were examined by plotting t/S vs. t for the HG₁, HG₂, HG₃, HG₄ and HG₅. Figure 2 shows the linear regression of the swelling curves obtained by means of Equation 4 for the P(AAm-co-AAc)/silver nanoparticles hydrogels in question. The initial swelling rate (r), the swelling rate constant (k_s) and the values of theoretical equilibrium swelling ($(S_{eq})_{max}$) of all hydrogels were calculated from the slope and the intersection of the lines. The results are presented in Table II.

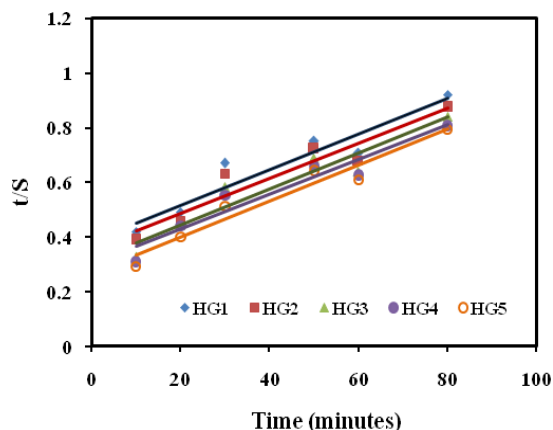


Figure 2: Swelling kinetic relations of P(AAm-co-AAc)/silver nanoparticles hydrogels at different ratios of AAm/AAc.

When a hydrogel is brought into contact with water, water diffuses and the hydrogel swells. Diffusion involves migration of water into pre-existing or dynamically formed spaces between hydrogel chains. Swelling of the hydrogel involves larger scale segmental motion resulting, ultimately, in an increased distance of separation between hydrogel chains. Analysis of the mechanisms of water diffusion in swellable polymeric systems is of prime importance due to applications of swellable polymers in the biomedical, pharmaceutical, environmental, and agricultural engineering fields. The swelling mechanism of the samples was determined by applying in the following equation [17]:

$$S \text{ (g/g)} = \frac{[W_t - W_0]}{W_0} = Kt^n$$

Where

K is the swelling constant and
 n is the swelling exponent calculated from the slopes of the lines of $\ln(S) - \ln(t)$ plots.

For cylindrical shapes, $n = 0.45-0.50$ and corresponds to Fickian diffusion, whereas $0.50 < n < 1.0$ indicates that diffusion is non-Fickian. This equation is applied to the initial stages of swelling and plots of $\ln(S)$ versus $\ln(t)$ yield straight lines. For the hydrogels, $\ln(S)$ versus $\ln(t)$ plots was drawn using the kinetics of swelling and some representative results are shown in Figure 3. The swelling exponents n were calculated from the slopes of the lines and are listed in Table II. The values of the diffusional exponent range are generally between 0.5405 and 0.6387. Hence, the diffusion of water into P(AAm-co-AAc)/silver nanoparticles hydrogels had a non-Fickian character. The value of n higher than 0.5 indicating diffusion of water to the interior of all the hydrogels, follows an anomalous mechanism. The anomalous behaviour of the hydrogel is due to the regularity of the chain and strong interaction via the formation of hydrogen bonding, leading to a compact structure which would prove the anomalous aspects of diffusion even for a molecule as small as water [17].

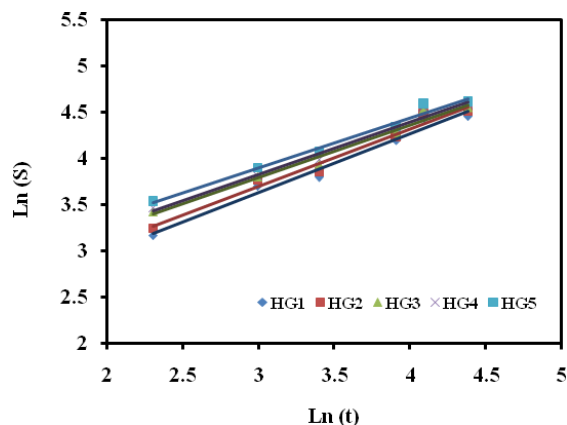


Figure 3: Swelling kinetic relations of P(AAm-co-AAc)/silver nanoparticles hydrogel at different ratios of AAm/AAc.

Non-Fickian diffusion processes have been thoroughly investigated [21-24]. Depending on the relative rates of chain relaxation and diffusion, non-Fickian diffusion has been classified into: "Case II transport" and "Anomalous transport" (Figure 4). Case II transport is dominated when the diffusion is very rapid compared to relaxation ($R_{diff} \gg R_{relax}$), with relaxation occurring at an observable rate. Here, the rate of mass uptake is directly proportional to time. The anomalous transport is observed when the diffusion and relaxation rates are comparable ($R_{diff} \approx R_{relax}$).

Since most polymers swell when they are in contact with certain solvents, Fick's laws should be applied with modified boundary conditions and/or a generalized diffusion coefficient to address the non-Fickian behavior. An explanation of the swelling mechanism of the prepared hydrogels through their non-fickian characteristics can be illustrated by the scheme represented in Figure 4 [25].

Table II: Some Swelling Parameters of P (AAm-co-AAc)/silver Nanoparticles Hydrogel.

Swelling parameter	AAm / AAc Ratio				
	100/0	70/30	50/50	30/70	0/100
$S_{exp.}$	86.9	91.4	95.4	98.9	100.4
S_{eq}	153.8	156.3	151.5	156.25	151.52
$K_s * 10^4$	1.0922	1.1422	1.3997	1.3585	1.6290
r	2.59	2.79	3.21	3.32	3.74
n	0.6387	0.6226	0.5698	0.5695	0.5405

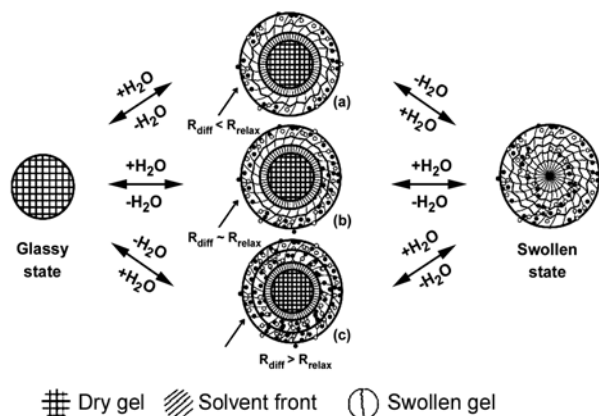


Figure 4: The mechanisms of Case II and anomalous diffusion.

3.2. Antimicrobial study

A recent study indicated that the bactericidal effect of silver nanoparticles mostly depends on the size of particles where silver nanoparticles having smaller sizes are more efficient and concluded that 1-10 nm have a direct interaction with bacteria [26]. The antibacterial activity is a manifestation of the release of silver nanoparticles from the Ag/PAAm-co-AAc hydrogel. Silver nanoparticles exhibit relatively large surface area, thus increasing their contact with bacteria or fungi. Silver nanoparticles show powerful bactericidal activity by binding with microbial DNA, thereby preventing bacterial replication.

P(AAm-co-AAc) hydrogel (HG₀) showed no inhibition zone. Results of the antimicrobial activity test against *Escherichia coli* (Gram -ve bacteria) and *Bacillus subtilis* (Gram +ve bacteria) showed that HG₃, HG₆ and HG₈ have an antibacterial activity while the HG₀ were generally inefficient. Table III represents the antimicrobial activity of the prepared hydrogels with different doses of silver nitrate upon

the selected bacteria and fungi, while figure 5 shows the growth of bacteria in a Petri dish containing hydrogels with different silver doses.

Table III: In vitro antimicrobial activity by agar method diffusion of tested materials

Sample in vials	<i>Candida albicans</i>	<i>Escherichia coli</i>	<i>Staphylococcus aureus</i>	<i>Bacillus subtilis</i>
HG ₀	-	-	-	--
HG ₃	+	+	+	+
HG ₆	+	+	+	+
HG ₈	+	++	++	++

+ve, zone of inhibition 10 mm or less

++ve, zone of inhibition 20 mm or less

-ve, no inhibition.

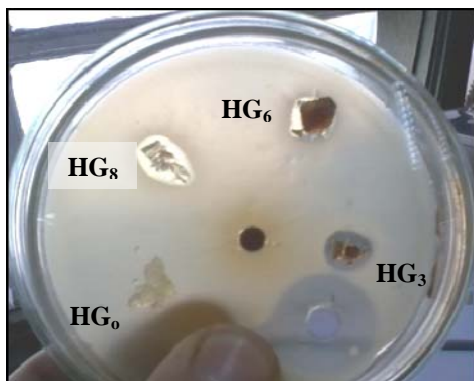


Figure 5: photograph showing the effect of nanocomposite upon bacterial activity

The same holds true for experiments carried out in parallel lines with fungi where silver nanoparticles derived from the prepared hydrogels show antifungal activity against *Candida albicans* as compared with the inactive blank sample HG₀.

The inhibition area follows the order: HG₈ > HG₆ > HG₃ as shown in Figure 9. This behaviour is expected where abundance and small sizes of silver nanoparticles (1-12 nm) in the prepared hydrogels are responsible for inhibition of bacterial and fungal growth.

3.3. Transmission Electron Microscopy

The size and morphology of silver nanoparticles formed on the P(AAm-co-AAc) hydrogel were determined through TEM imaging. Figure 6 represents a micrograph of a blank sample of, HG₀, of P(AAm-co-AAc) hydrogel in absence of silver nanoparticles.

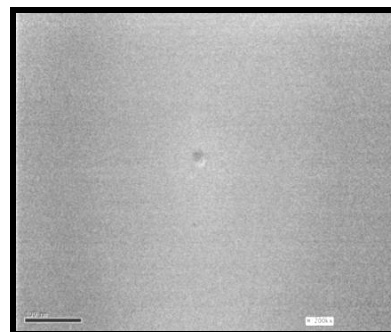


Figure 6: TEM micrograph of P(AAM-co-AAc) hydrogel

Figures 7-A, 8-A and 9-A represent images of micrographs for P(AAm-co-AAc) hydrogel/silver nanoparticles; referred here as HG₃, HG₆ and HG₈ using 0.01, 0.02 and 0.04 g silver nitrate respectively in preparation of these hydrogels. TEM micrographs revealed varieties in distribution of silver nanoparticles.

Careful examination of the images showed the silver nanoparticles with different variable sizes as well as smaller polydispersed particles. It should be noted, however, that the majority of the silver nanoparticles were scattered, a few of them showing aggregates indicating stabilization of the nanoparticles. The results represented by TEM images concluded that the particle size of individual nanoparticles seem to be 1-12 nm, whereas majority of silver nanoparticles exhibit smaller sizes.

Histograms of size distribution derived from TEM images for hydrogels HG₃, HG₆ and HG₈ are shown in figures 7-B, 8-B and 9-B. A detailed correlation between particle size and size distribution for each of these hydrogel systems is given below:

Figure 7-B shows the size range of silver nanoparticles formed on hydrogel; HG₃ prepared in presence of 0.01g silver nitrate. Sizes of these nanoparticles lie within the range 1-7 nm. TEM micrographs revealed also that a size range of 3-4 nm is prevailing. Size distribution of silver nanoparticles embedded in hydrogel HG₆ prepared under the action of 0.02 g silver nitrate as shown in Figure 8-B was found to be in the range of 1-12 nm. Nanoparticles having sizes ranging from 6-12 nm constitute the largest percentage within the specimen examined. Moreover, increasing the concentration of silver nitrate up to 0.04 g causes a considerable increase in the amount of silver nanoparticles with smaller sizes; 1-3 nm with some particles sized 4-5 nm and a low percentage of nanoparticles having sizes within the range of 6-12 nm. This is rather clarified by the data of the histogram represented in Figure 9-B.

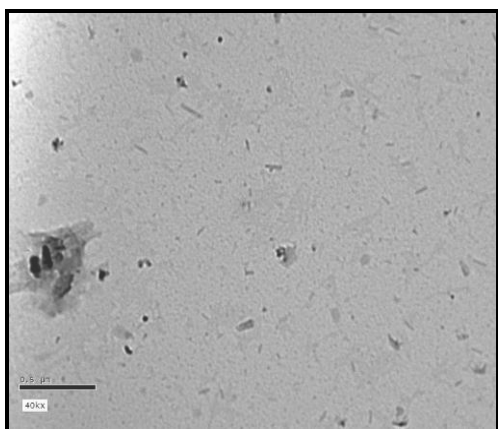


Figure 7-A: TEM micrograph of P(AAM-co-AAc)/silver nanoparticles hydrogel prepared using 0.01g AgNO_3

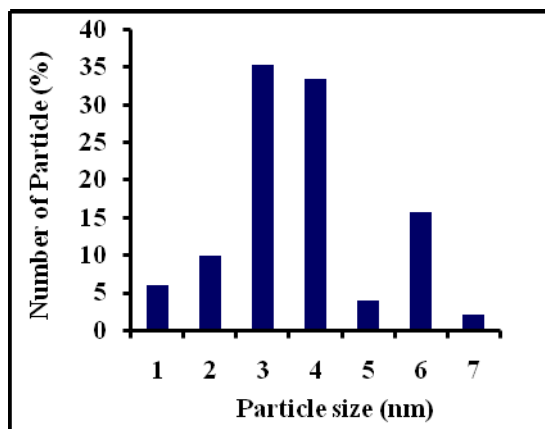


Figure 7-B: Histogram illustrating size distribution of silver nanoparticles via TEM micrograph of hydrogel prepared using 0.01g AgNO_3

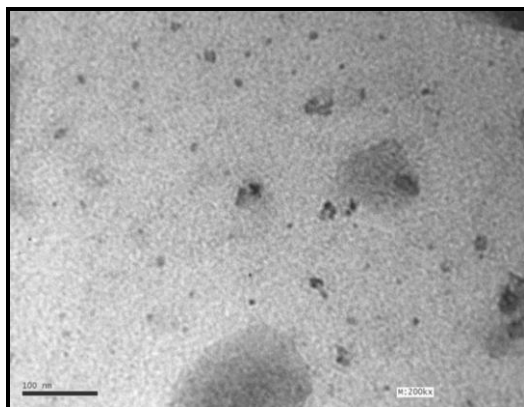


Figure 8-A: TEM micrograph of P(AAM-co-AAc)/silver nanoparticles hydrogel prepared using 0.02g AgNO_3

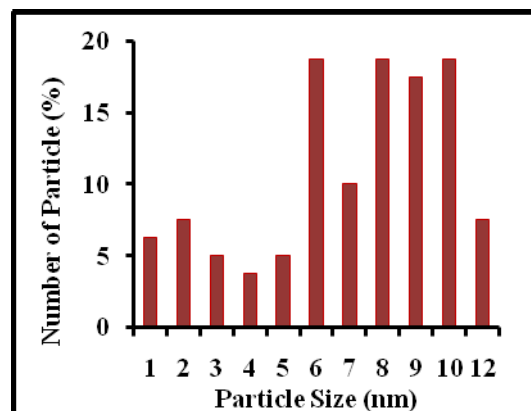


Figure 8-B: Histogram illustrating size distribution of silver nanoparticles via TEM micrograph of hydrogel prepared using 0.02 g AgNO_3

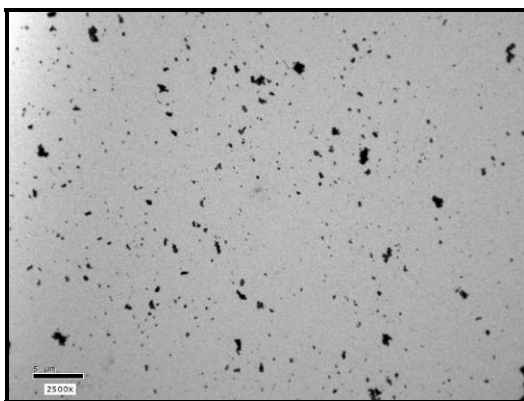


Figure 9-A: TEM micrograph of P(AAM-co-AAc)/silver nanoparticles hydrogel prepared using 0.04g AgNO_3

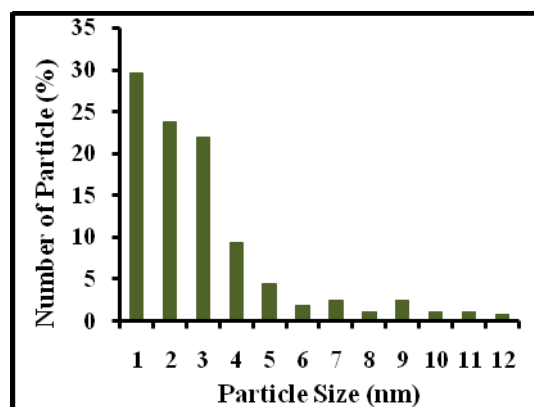


Figure 9-B: Histogram illustrating size distribution of silver nanoparticles via TEM micrograph of hydrogel prepared using 0.04 g AgNO_3

3.4. Antimicrobial activity and TEM micrographs

Correlation of the data of antimicrobial activity with those of TEM for hydrogels under investigation, conceive that both size and number of silver nanoparticles play an important role in the inhibition of bacterial and fungal growth. This can be exemplified by the study on sample HG₃ as shown by Figures 7-A and 7-B and Table III where low number and small size of silver nanoparticles resulted in a small inhibition zone, i.e. poor antimicrobial activity. Small sizes and larger number of silver nanoparticles observed with HG₆ sample, as shown in Figures 8-A and 8-B and Table III caused a slight improvement in bacterial and fungal inhibition.

On the other hand, hydrogel sample HG₈ exhibited a comparatively larger number of silver nanoparticles having widely distributed smaller particle sizes as illustrated by Figures 9-A and 9-B. The efficiency of this hydrogel sample to inhibit bacterial and fungal growth revealed a wide and distinct inhibition zone. This was confirmed by the data given in Table III.

It can be concluded that the results of TEM imaging of the prepared hydrogels are in accordance with those arrived at from the antimicrobial activities of these hydrogels.

4. Conclusion

P(AAm-co-AAc) hydrogels containing silver nanoparticles were successfully prepared via a free radical copolymerization, in presence of silver nitrate at varying doses along with concurrent, crosslinking and reduction of Ag⁺ ions to develop silver nanoparticles in the hydrogel matrix. The swelling capacities of the resulting hydrogels were evaluated. Swelling was found to be directly related to swelling duration and AAm/AAc ratio used in the polymerisation process. Kinetic studies of swelling concluded that the diffusion of these hydrogels was of the non-Fickian type. The hydrogel products were also characterized for size distribution of silver nanoparticles through examination of micrographs and histograms obtained using TEM. Antimicrobial activity of these hydrogels was also investigated. Correlation of TEM results with those of the hydrogel capability to inhibit bacterial and fungal growth was made and confirmed that small sizes and abundance of silver nanoparticles determine the antimicrobial activity of the hydrogel.

Corresponding author

Enas M. Ahmed¹

Department of Chemical Engineering & Pilot Plant
National Research Center, Dokki, Cairo, Egypt
elarefenas123@yahoo.com

5. References:

1. Kashyap, N., Kumar, N. and Kumar, M. Hydrogels for Pharmaceutica and Biomedical Applications, Critical Review in Therapeutic Drug Carrier Systems, 22(2005), p.107.
2. V. Thomas, Murali Mohan Yallapu, B. Sreedhar, S.K. Bajpai; A versatile strategy to fabricate hydrogel–silver nanocomposites and investigation of their antimicrobial activity, Journal of Colloid and Interface Science 315 (2007), p.389.
3. Q.L. Feng, F.Z. Cui, T.N. Kim, J.W. Kim, Ag-substituted hydroxyapatite coatings with both antimicrobial effects and biocompatibility J. Mater. Sci. Lett. 18 (1999), p. 559.
4. Lee, H.J., Yeo, S.Y., and Jeong, S.H., Antibacterial Effect of Nanosized Silver Colloidal Solution on Textile Fabrics, J. Mater. Sci., 38(2003), p.2199.
5. I. Margaret, S.L. Lui, V.K.M. Poon, I. Lung, A. Burd, Antimicrobial activities of silver dressings: an in vitro comparison, J. Med. Microbiol, 55 (2006), p.59.
6. John J. Curtin and Rodney M. Donlan, Using Bacteriophages To Reduce Formation of Catheter-Associated Biofilms by Staphylococcus epidermidis Antimicrob. Agents Chemother. 50 (2006), p.1268.
7. P. Jain, T. Pradeep, Biotechnology and Bioengineering Potential of silver nanoparticle-coated polyurethane foam as an antibacterial water filter, Prashant Jain and T.Pradeep, 90 (2005), p.59.
8. J. Zuhuang, patent number CN 1387700, 2003; M. Chen, S. Chen, patent number CN 1355335, 2002.
9. C.Wang, N.T. Flynn, R. Langer, Morphologically Well-defined Gold Nanoparticles Embedded in Thermo-Responsive Hydrogel Matrices Mater. Res. Soc. Symp. Proc. 820 (2004), R2.2.1.
10. Y. Murali. Mohan, T. Premkumar, K.J. Lee, K.E., Fabrication of Silver Nanoparticles in Hydrogel Networks, Geckeler, Macromol. Rapid Commun. 27 (2006), p.1346.
11. Grier, N, "Silver and Its Compounds," In: Disinfection, Sterilization and Preservation, edited by S. Block, Lea & Febiger, Philadelphia, (1983), p. 375.
12. M. Kowshik, S. Ashtaputre, S. Kharrazi, W. Vogel, J. Urban, SK. Kulkarni, KM. Paknikar: Extracellular synthesis of silver

- nanoparticles by a silver-tolerant yeast strain MKY3. *Nanotechnology* 14 (95) (2003) p. 100.
13. N. Duran, P.D. Marcato, O.L. Alves, G. Souza, Mechanistic aspects of biosynthesis of silver nanoparticles by several *Fusarium oxysporum* strains. *Journal of Nanotechnology* 3 (2005), p.8.
 14. Lehninger Principles of Biochemistry, 3rd ed.; By David L. Nelson and Michael M. Cox. Worth Publishers: New York, 2000. ISBN 1-57259-9316. 1255 pp.
 15. A.B. Lansdown, Silver in health care: antimicrobial effects and safety in use *Current Problems in Dermatology* 33 (17) (2006), p.34.
 16. A. Chakravarti, S. Gangodawila, M.J. Long, N.S. Morris, A.R. Blacklock, D.J. Stickler, An Electrified Catheter to Resist Encrustation by *Proteus Mirabilis* Biofilm. *Journal of Urology* 174 (1129) (2005), p. 32.
 17. Enas M. Ahmed, Fatma S. Aggor. Swelling kinetic study and characterisation of crosslinked Hydrogel containing Silver Nanoparticles. *J. Appl. Polym. Sci.* 117(2010), p.2168.
 18. Tuncer Caykara, Simin kipper, Gokhan Demirel, Thermosensitive poly(N-isopropylacrylamide-co-acrylamide) hydrogels: synthesis, swelling and interaction with ionic surfactants, *European polymer. J.* 42(2005), p.348.
 19. R. Cruickshank, J.P. Duguid, B.P. Marion, R.H.A. Swain, *Medicinal Microbiology*, 12th ed., vol. II, Churchill Livingstone, London,(1975), p. 196.
 20. Bajpai, S.K., Mohan, Y. M., Bajpai, M., Tankhiwale, R., & Thomas, V. Synthesis of polymer stabilized silver and gold nanostructures. *Journal of nanoscience and nanotechnology*, 7(2007), p. 2994.
 21. Liu Q, Wang X, Kee DD, Mass transport through swelling membranes, *Int J Eng Sci*, 43(2005), p.1464.
 22. Vrentas JS, Vrentas CM, Steady viscoelastic diffusion, *J Appl Polym Sci*, 88(2003), p.3256.
 23. Afif AE, Grme M, Non-Fickian mass transport in polymers, *J Rheol*, 46 (2002), p. 591.
 24. Rajagopa KR, Diffusion through polymeric solids undergoing large deformations, *Mater Sci Tech*, 19(2003), p.1175.
 25. Rossi G, Mazich KA, Kinetics of swelling for a cross-linked elastomer or gel in the presence of a good solvent, *Phys Rev A*, 44 (1991), p.4793.
 26. Morones, J.R., Elechiguerra, J.L., Camacho, A., Holt, K., Kouri, J.B., Ramirez, J.P., & Yacaman M.J. The bactericidal effect of silver nanoparticles. *Nanotechnology*, 16(2005), p.2346.

7/1/2010